Am J Physiol Cell Physiol 309: C736–C746, 2015.
First published October 7, 2015; doi:10.1152/ajpcell.00050.2015.

CALL FOR PAPERS | *Cell and Molecular Processes in Cancer Metastasis*

Lamin A/C deficiency reduces circulating tumor cell resistance to fluid shear stress

Michael J. Mitchell,[1] Celine Denais,[1,2] Maxine F. Chan,[1] Zhexiao Wang,[1] Jan Lammerding,[1,2] and Michael R. King[1]

[1]*Nancy E. and Peter C. Meinig School of Biomedical Engineering, Cornell University, Ithaca, New York; and* [2]*Weill Institute for Cell and Molecular Biology, Cornell University, Ithaca, New York*

Submitted 19 February 2015; accepted in final form 17 September 2015

Mitchell MJ, Denais C, Chan MF, Wang Z, Lammerding J, King MR. Lamin A/C deficiency reduces circulating tumor cell resistance to fluid shear stress. *Am J Physiol Cell Physiol* 309: C736–C746, 2015. First published October 7, 2015; doi:10.1152/ajpcell.00050.2015.—Metastasis contributes to over 90% of cancer-related deaths and is initiated when cancer cells detach from the primary tumor, invade the basement membrane, and enter the circulation as circulating tumor cells (CTCs). While metastasis is viewed as an inefficient process with most CTCs dying within the bloodstream, it is evident that some CTCs are capable of resisting hemodynamic shear forces to form secondary tumors in distant tissues. We hypothesized that nuclear lamins A and C (A/C) act as key structural components within CTCs necessary to resist destruction from elevated shear forces of the bloodstream. Herein, we show that, compared with nonmalignant epithelial cells, tumor cells are resistant to elevated fluid shear forces in vitro that mimic those within the bloodstream, as evidenced by significant decreases in cellular apoptosis and necrosis. Knockdown of lamin A/C significantly reduced tumor cell resistance to fluid shear stress, with significantly increased cell death compared with parental tumor cell and nontargeting controls. Interestingly, lamin A/C knockdown increased shear stress-induced tumor cell apoptosis, but did not significantly affect cellular necrosis. These data demonstrate that lamin A/C is an important structural component that enables tumor cell resistance to fluid shear stress-mediated death in the bloodstream, and may thus facilitate survival and hematogenous metastasis of CTCs.

cancer; metastasis; lamin; fluid shear stress; apoptosis

METASTASIS IS THE CAUSE OF ~90% of cancer-related deaths (9, 39). This phenomenon is initiated when cancer cells detach from the primary tumor, invade surrounding tissue, and subsequently enter the bloodstream as circulating tumor cells (CTCs) during the process of intravasation (64). CTCs must survive immunological stress and hemodynamic shear forces to translocate through the bloodstream to microvessels in anatomically distant organs (28, 46, 47). In the circulation, CTCs interact with the receptor-bearing endothelial cell wall via selectin-mediated rolling and cell arrest (9, 11, 15). CTCs then firmly adhere to the endothelial cell wall and exit the bloodstream in a process known as extravasation, survive within surrounding tissue, and proliferate to form secondary tumors (9, 48). Surgery, radiation, and chemotherapy have proven effective at treating primary tumors; however, the difficulty in treating and detecting metastases typically signals a poor patient prognosis (46). Although the majority of CTCs die within the circulation (10, 21, 37), it is evident that a small population of CTCs are capable of surviving transit through the circulation to form metastases. Thus numerous approaches are currently under development to isolate CTCs from the bloodstream to develop personalized medicine regimens (29, 42, 43) and technologies to target and kill CTCs within the bloodstream before metastasis formation (41, 44, 50).

Fluid shear stress (FSS) is one of the key physical forces that can affect the viability of tumor cells (40, 47, 64). In the tumor microenvironment, tumor cells are exposed to FSS generated by slow interstitial flows, the movement of fluid around cells and through the extracellular matrix (ECM) of the interstitium (56, 57). In the presence of interstitial flow, tumor cells are exposed to FSS on the order of 0.1 dyn/cm^2 (53, 58). In the bloodstream, the FSS to which tumor cells are exposed increases significantly, ranging from 0.5 to 4.0 dyn/cm^2 in the venous circulation and 4.0 to 30.0 dyn/cm^2 in the arterial circulation (60). Shear rates can range from 160 s^{-1} within veins to 900 s^{-1} within arteries. Tumor cells transiently encounter even greater FSS in turbulent flows within the heart, near the endothelial cell wall of large vessels, and at large vessel bifurcations, where FSS is on the order of >1,000 dyn/cm^2 (12, 38, 55). Elevated FSS and shear rates have been shown to affect circulating cancer cell viability, which can thus affect the probability of metastasis formation. Exposure to FSS in a cone-and-plate viscometer at shear rates >300 s^{-1} induced a significant loss of melanoma cell viability (6). Initial in vivo studies demonstrated metastasis of CTCs through the circulation to be an inefficient process, with the majority of intravenously injected tumor cells dying within 24 h and minimal CTCs forming metastases (21, 65). Despite this, it is evident that subpopulations of CTCs are capable of withstanding elevated FSS within the bloodstream to form secondary tumors. However, there have been few studies investigating the cellular structural properties that allow tumor cells to withstand FSS.

Recent work has investigated the tumor cell plasma membrane as a key structural component in tumor cell resistance to elevated FSS as high as 6,000 dyn/cm^2 (3). While FSS has been previously shown to disrupt plasma membrane integrity (13, 59), recent work has shown that tumor cells are capable of repairing FSS-induced plasma membrane damage in a calcium-dependent manner (3). Plasma membrane repair and resistance to such FSS-induced damage was shown to increase with

Address for reprint requests and other correspondence: M. R. King, Meinig School of Biomedical Engineering, Cornell Univ., 205 Weill Hall, 237 Tower Rd., Ithaca, NY 14853 (e-mail: mike.king@cornell.edu).

increased FSS exposure (3). In addition to the plasma membrane, the nuclear lamina is a key structural component of tumor cells and has been shown to play a key role in tumor progression and metastasis (18). In particular, nuclear lamins A and C (A/C) provide structural integrity to the nucleus (32, 33), are critical in physically connecting the cytoskeleton to the nucleus, and enable mechanical forces to be transmitted from the ECM and cytoskeleton to nuclear components of the cell (22, 36, 51, 67). Cells that lack lamin A/C show reduced nuclear stiffness and increased nuclear fragility, which leads to increased cell death on exposure to mechanical forces and contributes to a variety of diseases (17, 24, 33). In cancer, A-type lamins have been found to be upregulated in prostate, skin, and ovarian tumors (23, 27, 30, 34) and could play a role in providing mechanical stability to tumor cells in the circulation during metastasis. On the other hand, lamins A/C are downregulated in many lymphomas, small cell lung cancer, and in breast cancer (8, 18), and reduced levels of lamin A/C negatively correlate with disease-free survival in breast cancer (61). Reduced levels of lamin A/C and the associated increased nuclear deformability could facilitate migration of metastatic cancer cells through dense ECM and tight interstitial spaces (16, 24). However, it is currently unknown whether lamin A/C contributes to tumor cell support against forces such as FSS within the circulation. In this study, we compared the ability of tumor cells and epithelial cells to withstand FSS-induced cell death in vitro via perfusion of cell suspensions through microscale conduits at elevated FSS that was transiently experienced by tumor cells in the in vivo circulation. To assess the role of lamin A/C in potentially maintaining mechanical stability and viability of CTCs within the bloodstream, we measured rates of FSS-induced cell death in metastatic breast cancer cells depleted for lamin A/C via short hairpin RNA (shRNA) and small interfering RNA (siRNA).

MATERIALS AND METHODS

Cell culture. Breast adenocarcinoma cell lines MDA-MB-231 [American Type Culture Collection (ATCC) no. HTB-26] and MDA-MB-468 (ATCC no. HTB-132), and non-tumorigenic mammary epithelial cell line MCF10A (ATCC no. CRL-10317) were purchased from ATCC (Manassas, VA). MDA-MB-231 and MDA-MB-468 cells were cultured in Dulbecco's modified Eagle's medium (DMEM; Invitrogen) supplemented with 10% (vol/vol) fetal bovine serum (FBS; Invitrogen, San Diego, CA) and 1% (vol/vol) PenStrep (Invitrogen). MCF10A cells were cultured in DMEM (Invitrogen) supplemented with 5% horse serum (Atlanta Biologicals, Norcross, GA), 1% PenStrep, 0.5 mg/ml hydrocortisone (Sigma Aldrich, St. Louis, MO), 20 ng/ml human epidermal growth factor (Invitrogen), 10 ng/ml bovine insulin (Sigma), and 100 ng/ml cholera toxin (Enzo Life Sciences, Farmingdale, NY). MDA-MB-231, MDA-MB-468, and MCF10A cells were cultured under humidified conditions at 37°C and 5% CO_2 and were not allowed to exceed 90% confluence. Before FSS pulse assays, tumor and epithelial cells were dislodged from plates using trypsin-EDTA (Invitrogen), subjected to centrifugation (125 *g*) for 5 min, and resuspended at a concentration of 0.5×10^6 cells/ml in Hank's balanced salt solution (HBSS) containing 0.5% human serum albumin, 2 mM Ca^{2+}, 1 mM Mg^{2+}, and 10 mM HEPES (Invitrogen), buffered to pH 7.4.

Mononuclear leukocyte isolation. Mononuclear leukocytes were isolated from human peripheral blood using a previously described protocol (7, 45, 49). All human subject protocols were approved by the Institutional Review Board for Human Participants of Cornell University. Briefly, human peripheral blood was obtained from healthy blood donors after informed consent via venipuncture and collected using sterile sodium heparin-containing tubes (BD Biosciences, San Jose, CA). Leukocytes were isolated from blood by centrifugation at 480 *g* for 50 min at 23°C, in a Marathon 8K centrifuge (Fisher Scientific, Pittsburgh, PA) using 1-Step Polymorphs (Accurate Chemical & Scientific, Westbury, NY). Leukocytes were extracted and washed in Ca^{2+} and Mg^{2+}-free HBSS, and all remaining red blood cells in the suspension were lysed hypotonically. Leukocytes were resuspended at a concentration of 0.5×10^6 cells/ml in HBSS containing 0.5% human serum albumin, 2 mM Ca^{2+}, 1 mM Mg^{2+}, and 10 mM HEPES (Invitrogen), buffered to pH 7.4, before FSS pulse assays.

Generation of shRNA lamin A/C knockdown MDA-MB-231 cell lines. Lentiviral particles were produced using the HEK 293-TN cell line (System Biosciences, Mountain View, CA), which was transformed with the SV40 large T antigen to promote robust growth and displayed the Neomycin resistance marker for stable propagation. Briefly, lentiviral packaging plasmids (ENV, Pol, GAG) were cotransfected with mission shRNA vector purchased from Sigma (lentivirus plasmid vector pLKO.1-Puro containing shRNA targeting sequence of lamin A/C, clone no. NM_170707.1-752s1c1, or a nontargeting control sequence) using PureFection nanotechnology-based transfection reagent (System Biosciences). Media (DMEM containing pyruvate + 10% FBS) was changed the next day and replaced by MEM + 10% FBS without PenStrep. Lentivirus-containing supernatants were collected at 48 and 72 h after transfection, filtered through a 0.45-μm filter, and used as the viral stock.

MDA-MB-231 cells were seeded into six-well plates so that they reached 50–60% confluency on the day of infection. Cells were transduced at least 3 consecutive days with the viral stock in the presence of 8 μg/ml freshly prepared polybrene (Sigma). The viral solution was removed, and cells were allowed to incubate in fresh medium an additional 24 h before being subcultured. The cells were then subjected to stringent selection, i.e., positive cells were selected for 1 wk in growth medium containing 10 μg/ml of puromycin (Sigma). Clonal cell populations were generated by serial dilution of the positively selected stable knockdown of lamin A/C.

Generation of siRNA lamin A/C knockdown MDA-MB-231 and MDA-MB-468 cell lines. siRNA oligonucleotides targeting human LMNA (ON-TARGET plus SMART pool, L-004978-00) and negative control siRNA (ON-TARGET plus non-targeting pool, D-001810-10) were purchased from Dharmacon (GE Healthcare). MDA-MB-231 and MDA-MB-468 cells were seeded into six-well plates using optimized density the day before treatment. Cells were transfected with the siRNAs using DharmaFECT transfection reagents according to the manufacturer's instructions at a final concentration of 25 nM. After transfection, the cells were harvested at 72 h for protein extraction and additional analysis.

Western blot and immunofluorescence. Cells were collected and counted for total cell lysate preparation. Homogenization of the same number of cells was performed in 200 μl of Laemmli buffer containing 0.3 M of dithiothreitol using the 29G needle shearing method, and lysates were boiled for 5 min at 95°C. Lamin A/C expression was detected via Western blot using a goat anti-human lamin A/C N18 antibody (1:2,000 dilution) (Santa Cruz Biotechnology, Santa Cruz, CA), and tubulin expression was detected using a mouse anti-human tubulin T5168 antibody (1:2,000 dilution) (Sigma), with both antibodies diluted in 5% milk.

For immunofluorescence studies, cells were grown on 20 μg/ml fibronectin-coated glass coverslips before treatment. Seventy-two hours after siRNA transfection, the coverslips were washed once with phosphate-buffered saline and fixed in 4% paraformaldehyde for 15 min at room temperature (RT). Cells were stained for lamin A/C, and B1 were detected via immunofluorescence using a mouse anti-human lamin A/C JOL2 antibody (ab40567; Abcam, Cambridge, MA) and rabbit anti-human lamin B1 antibody (ab16048; Abcam), respectively, both at a 1:400 dilution (into 3% BSA). Nuclei were counterstained

with Hoechst 33342 (dilution 1:1,000; Life Technologies). The coverslips were then mounted on slides and viewed on a Zeiss LSM 700 confocal microscope.

FSS pulse assay. Leukocytes, tumor cells, and epithelial cell lines were exposed to pulses of elevated FSS in vitro using a modified form of a previously described protocol (3). Elevated FSS pulses mimic the flow environment that CTCs transiently encounter in vivo near the walls of large vessels, within turbulent flow of the heart, or at large vessel bifurcations (55). Poiseuille's equation ($\tau = 4Q\mu/\pi R^3$) was used to calculate FSS exposure, where τ is the wall shear stress (WSS) in dyn/cm^2; Q is flow rate in cm^3/s; μ is the viscosity of the medium [HBSS buffer treated as water at n(RT); 0.01 dyn·s·cm^2]; and R is the radius of the needle (30 G average internal radius = 7.94×10^{-3} cm), which acts as a microscale conduit. FSS exposure time was determined by dividing the volume of the needle by the given flow rate (14 ml/min). At a flow rate of 14 ml/min, the WSS is calculated to be 5,920 dyn/cm^2, and the FSS exposure time is 1.08 ms. Note that, within the conduit, the local shear stress varies linearly with radial position, from a maximum at the wall to zero at the centerline. Thus cells randomly dispersed across all streamlines would experience an average local shear stress equal to two-thirds of the WSS value (31). In the absence of detailed information of the streamline distribution of entering cells, and to maintain consistency with previous studies of tumor cell response to FSS (47), we quote the calculated WSS value here. Viability measurements were expressed as a function of WSS. Cell suspensions were dilute enough (~0.2% volume fraction) to be described as Poiseuille flow. To assess for laminar flow conditions throughout the FSS pulse assay, Reynolds number (Re) was calculated using the equation $Re = \rho v D/\mu$, where ρ is the density of buffer, treated as water at RT (0.998 g/cm^3), v is the velocity of flow, D is the diameter of the needle, and μ is the dynamic viscosity of the flow buffer. The Re at a flow rate of 14 ml/min (~1,850) did not exceed the Re threshold for laminar flow (2,200).

Before FSS exposure, all cells were incubated in 2 μM of a calcein-AM fluorescent viability dye (Invitrogen) for 15 min at RT, as per manufacturer's instructions. Some cell suspensions were not labeled with calcein-AM, to allow for later cellular apoptosis and necrosis detection using a fluorescent annexin-V/propidium iodide (PI) assay. Ten milliliters of suspensions of individual cell types (0.5×10^6 cells/ml) were placed into 50-ml polypropylene tubes (VWR International, Bridgeport, NJ) and loaded into a 10-ml syringe (BD Biosciences, San Jose, CA) by drawing the suspension manually, in the absence of an attached needle. All syringes and needles were treated with 5% BSA in phosphate-buffered saline before shear assays were conducted, to minimize the number of cells lost due to adhesion to the syringe and needle walls. Aliquots (1 ml) of cell suspension were gently expelled from the syringe and retained to account for viability changes due to syringe contact and served as controls that were not exposed to FSS. Cells were then exposed to brief pulses of elevated FSS via perfusion through microscale conduits using a high-pressure PHD2000 syringe pump (Harvard Apparatus, South Natick, MA). Cell suspensions were expelled at a constant flow rate (14 ml/min) at RT, and collected in tubes placed at a 45° angle at the tip of the needle. Cells were maintained within tubes for 90 s after collection, to mimic in vivo conditions in which cells were transiently exposed to elevated FSS, before the process was then repeated to expose cells to a range of 2–10 pulses of elevated FSS. Aliquots (1 ml) of cell suspension were collected across the range of FSS pulses for later viability measurements. Cell suspensions that were not exposed to FSS, which had been in suspension for the entire duration of the assay, were sampled and treated as 100% viability controls. All aliquots were centrifuged, resuspended in media, and incubated under humidified conditions at 37°C and 5% CO_2 either overnight (for calcein-AM mediated viability measurements) or for 2 h (for annexin-V/PI assays).

Flow cytometry viability assays. After overnight incubation, viability of FSS- and non-FSS-exposed cells was determined by measuring the number of cells positive for fluorescent calcein-AM staining using an Accuri C6 flow cytometer. The number of FSS-exposed calcein-AM$^+$ cells was divided by the number of cells in non-FSS-exposed control samples to determine percent viability. To determine the mode of cell death via flow cytometry, samples were incubated for 2 h post-FSS exposure and then labeled with an annexin-V/PI viability assay. The complete cell samples (floating and adherent cells) were recovered, prepared, and processed via flow cytometry per the manufacturer's instructions. Briefly, cells were classified into four cate-

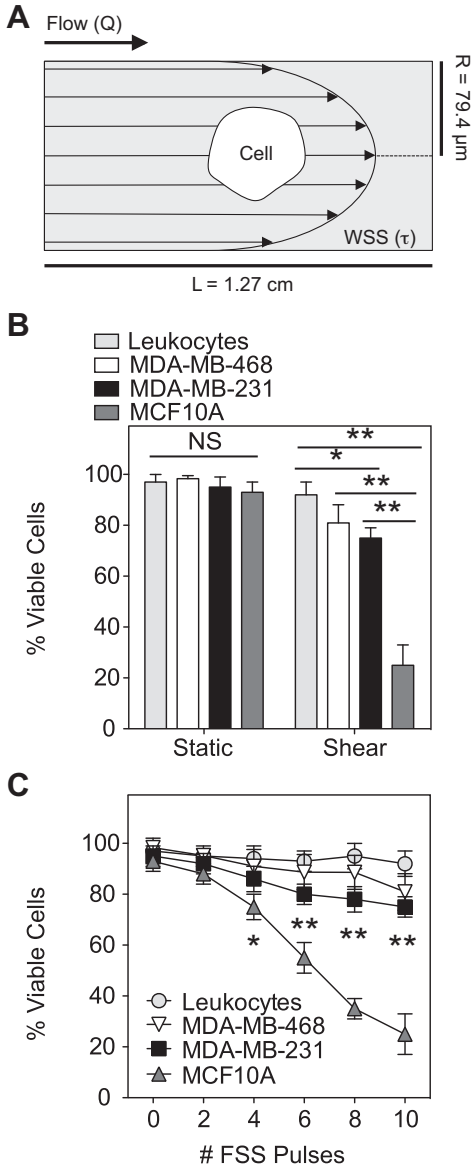

Fig. 1. Tumor cells resist fluid shear stress (FSS)-induced cell death to a greater extent than nonmalignant epithelial cells. *A*: schematic of microscale conduit used to expose cells in suspension to millisecond pulses of elevated FSS. WSS, wall shear stress; *L*, length of microscale conduit; *R*, radius of microscale conduit. *B*: percentage of viable leukocytes, tumor cells (MDA-MB-231 and MDA-MB-468), and nonmalignant epithelial cells (MCF10A) after exposure to static conditions (static) or 10-ms pulses of FSS (shear). All cell types were labeled with a cell viability dye (calcein-AM), exposed to elevated FSS, and immediately placed back into culture for ~18 h. Viability was determined via flow cytometry by counting the number of cells expressing calcein-AM. WSS = 5,920 dyn/cm^2. *C*: dose response of cells to FSS. Cell types were exposed to 0–10 pulses of FSS. Values are means ± SE for three independent measurements. *$P < 0.05$. **$P < 0.01$. NS, not significant.

gories based on dye uptake: viable cells (negative for annexin-V and PI), early-apoptotic cells (positive for annexin-V only), late-apoptotic cells (positive for annexin-V and PI), and necrotic cells (positive for PI only). Gates were determined based on viable, untreated cell controls.

Statistical analysis. Where appropriate, Student *t*-test and one-way ANOVA with Tukey posttest comparing all means were used at a significance level of $\alpha = 0.05$. All statistical analyses were performed using GraphPad Prism 5.0c for Mac OS X (GraphPad software) and Kaleidagraph (Synergy) software.

RESULTS

Tumor cells resist FSS-induced cell death compared with nonmalignant epithelial cells. To determine the effects of elevated FSS pulse exposure on tumor cells, epithelial cells, and leukocytes, we utilized a microfluidic protocol consisting of a high-pressure syringe pump to perfuse cell suspensions through microscale conduits (Fig. 1*A*). We utilized this protocol to generate an elevated level of FSS comparable to that experienced by cells within areas of the circulation, including vessel bifurcations, turbulent flow within the heart, and near the walls of large vessels (38, 55). The millisecond pulses of FSS are within the physiological range, as numerous studies have estimated elevated FSS pulses in heart valves to be within a range of 1–30 ms (1, 4, 14). Using this protocol, we exposed calcein-AM labeled primary human mononuclear leukocytes, breast cancer cells (MDA-MB-231 and MDA-MB-468), and normal mammary epithelial cells (MCF10A) to pulses of elevated FSS and assessed their viability after 10 FSS pulses (Fig. 1*B*). All cell types remained generally viable (>95%) under static conditions in suspension, as determined using calcein-AM staining and flow cytometry quantification. However, tumor cells were significantly more viable (~75%) than nontransformed breast epithelial cells (~25%) after exposure to 10 pulses of elevated FSS (Fig. 1*B*). Both cell types were significantly less viable than human leukocytes (~90%), which reside in the circulation and are regularly exposed to elevated FSS. Control experiments were performed to establish that the loss of cell viability observed in this protocol is a result of exposure to FSS and not a function of other variables. It is important to note that these changes in viability are not due to cell detachment, anoikis, or changes in temperature, as control samples not exposed to FSS were in suspension for the same duration of time as cells exposed to FSS, were also detached from culture surfaces, exposed to RT, and yet did not exhibit changes in cell viability over the course of the experiment (Fig. 1*B*). The results are consistent with previous work with cells of a different epithelial origin, showing that the prostate cancer cell line PC-3 is more resistant to FSS-induced cell death than nonmalignant prostate cell lines PWR-1E and RWPE-1 (3). These data suggest that breast cancer cells are resistant to elevated

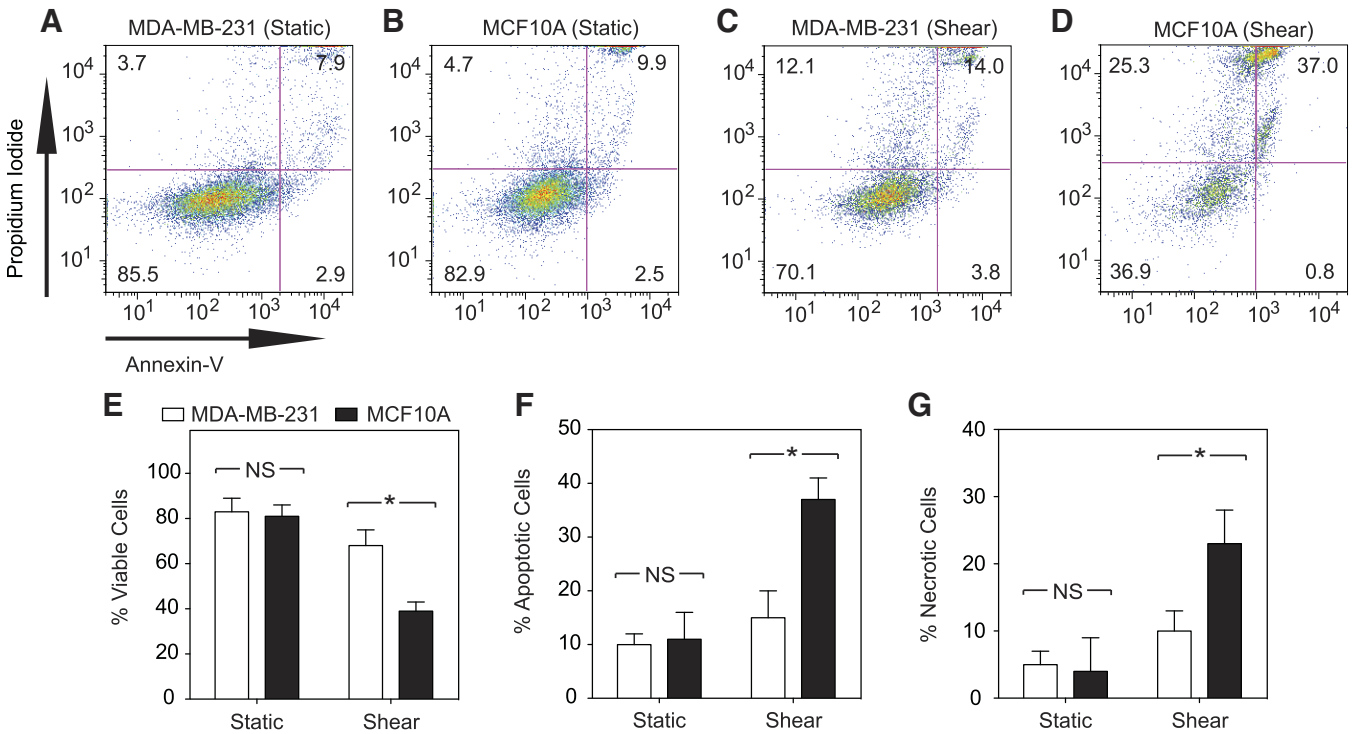

Fig. 2. Decreased apoptosis and necrosis in malignant MDA-MB-231 cells compared with nonmalignant MCF10A cells after FSS exposure. Cells were exposed to 10 pulses of high FSS (WSS: 5,920 dyn/cm^2), placed into culture for 2 h, and assessed for apoptosis and necrosis using annexin-V/propidium iodide (PI) assay. *A–D*: annexin-V/PI flow cytometry plots of MDA-MB-231 (*A* and *C*) and MCF10A (*B* and *D*) cells exposed to static conditions (*A* and *B*) and millisecond pulses of FSS (*C* and *D*). *Bottom left* quadrant (annexin-V negative, PI negative) denotes viable cells. *Top left* quadrant (annexin-V negative, PI positive) denotes necrotic cells. *Bottom right* quadrant (annexin-V positive, PI negative) denotes early-apoptotic cells. *Top right* quadrant (annexin-V positive, PI positive) denotes late-apoptotic cells. *E*: percentage of viable MDA-MB-231 and MCF10A cells after exposure to static conditions (static) or 10 pulses of elevated FSS (shear). *F*: percentage of apoptotic MDA-MB-231 and MCF10A cells after exposure to static conditions (static) or 10 pulses of elevated FSS (shear). *G*: percentage of necrotic MDA-MB-231 and MCF10A cells after exposure to static conditions (static) or 10 pulses of elevated FSS (shear). Values are means ± SE of three independent measurements. *$P < 0.05$.

shear forces within the bloodstream, compared with nonmalignant mammary epithelial cells.

Tumor cell resistance to cell death is FSS pulse dependent. To assess the effect of the number of FSS pulses on tumor cell resistance to cell death, leukocytes, MDA-MB-231 and MDA-MB-468 cancer cells, and MCF10A epithelial cells were exposed to a number of FSS pulses, ranging from 2–10 pulses, with 90 s in between consecutive pulses, and subsequently assessed for viability via calcein-AM dye retention and flow cytometry quantification. No significant differences in cell viability were observed between all cell types after exposure to two pulses of elevated shear stress (Fig. 1*C*). However,

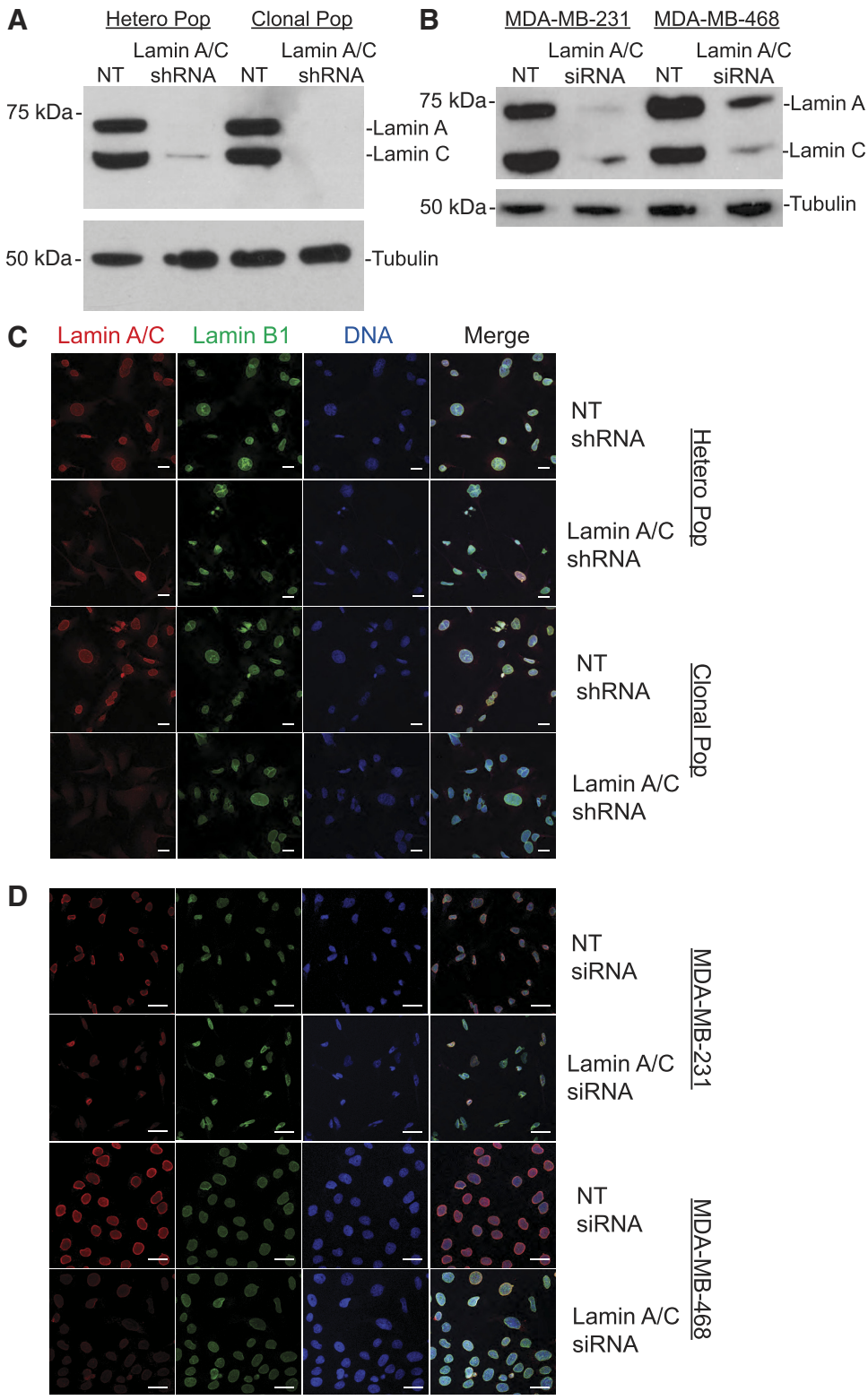

Fig. 3. Short hairpin RNA (shRNA)- and small interfering RNA (siRNA)-mediated knockdown (KD) of lamins A and C (A/C) in MDA-MB-231 and MDA-MB-468 breast cancer cells. *A*: Western blot of lamin A/C expression in clonal (Clonal Pop) [nontarget control (NT) and lamin A/C shRNA KD] and heterogeneous (NT and lamin A/C shRNA KD) populations (Hetero Pop) of MDA-MB-231 cells. *B*: Western blot of lamin A/C expression in MDA-MB-231 and MDA-MB-468 cells after treatment with NT and lamin A/C siRNA. *C*: fluorescence micrograph images of lamin A/C, lamin B1, and DNA in Clonal Pop and Hetero Pop of MDA-MB-231 cells after treatment with NT and lamin A/C shRNA. *D*: fluorescence micrograph images of lamin A/C, lamin B1, and DNA in MDA-MB-231 and MDA-MB-468 cells after treatment with NT and lamin A/C siRNA. Scale bar: 10 μm.

MCF10A epithelial cells were significantly less viable than MDA-MB-231 tumor cells after exposure to four pulses of elevated FSS (Fig. 1*C*). MCF10A viability significantly decreased as the number of FSS pulses increased to 10 (<25% viability), while MDA-MB-231 and MDA-MB-468 breast cancer cells remained significantly higher in terms of viability (>75%).

Increased cellular apoptosis and necrosis after exposure to FSS pulses. FSS effects on cellular apoptosis and necrosis have previously been examined in endothelial cells and osteoblasts

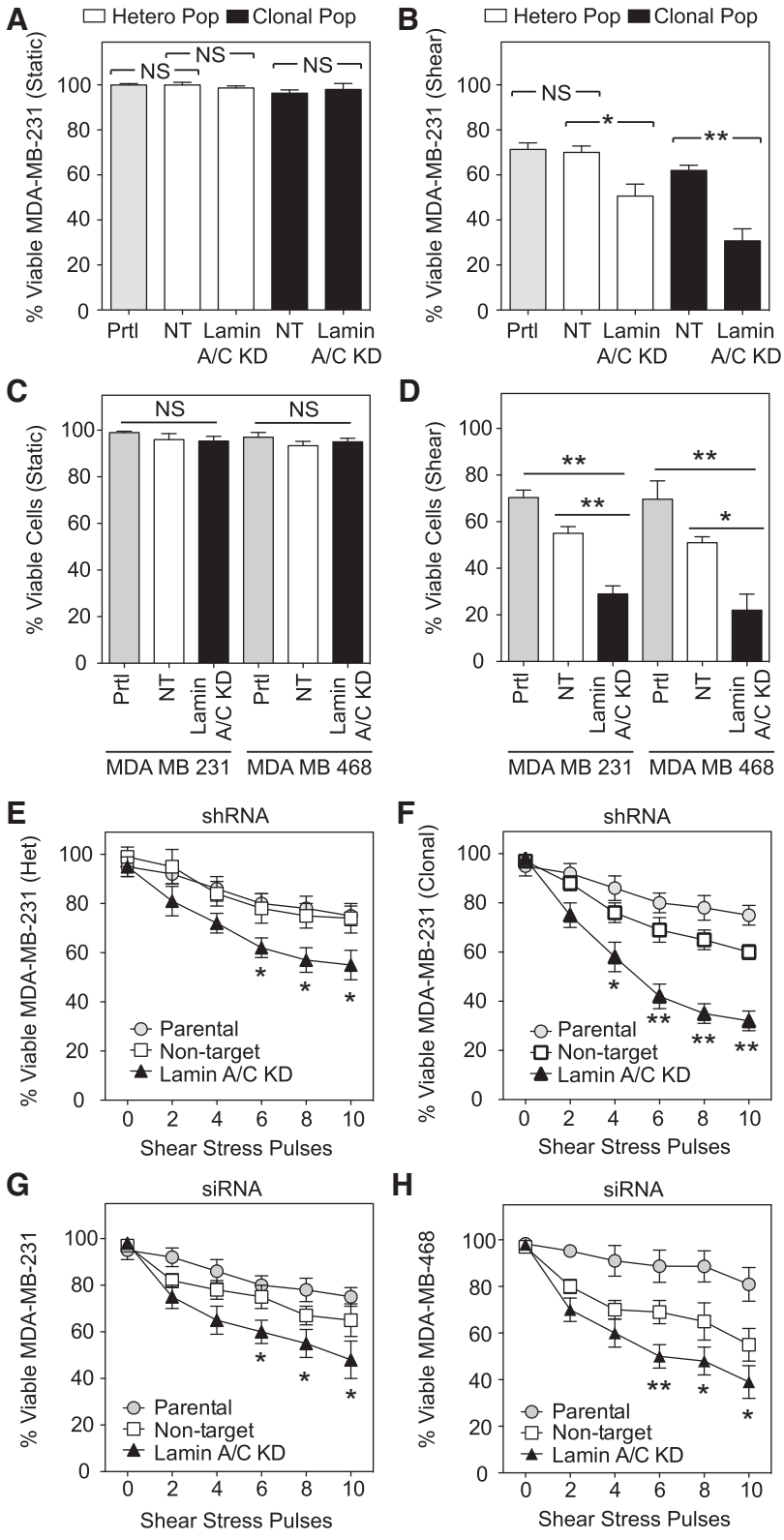

Fig. 4. Lamin A/C deficiency reduces tumor cell resistance to FSS-induced cell death in a FSS dose-dependent manner. *A* and *B*: percentage of viable parental (Prtl) MDA-MB-231 and lamin A/C deficient (shRNA-mediated) MDA-MB-231 tumor cells after exposure to static conditions (*A*) or 10-ms pulses of FSS (*B*). *C* and *D*: percentage of viable lamin A/C deficient (siRNA-mediated) MDA-MB-231 and MDA-MB-468 tumor cells after exposure to static conditions (*C*) or 10-ms pulses of FSS (*D*). *E*: dose response of Prtl and Hetero (Het) (NT and lamin A/C shRNA KD) populations of MDA-MB-231 cells to FSS. *F*: dose response of Prtl populations and Clonal Pop (NT and lamin A/C shRNA KD) of MDA-MB-231 cells to FSS. *G*: dose response of MDA-MB-231 (Prtl, NT, and lamin A/C siRNA KD) cell populations to FSS. *H*: dose response of MDA-MB-468 (Prtl, NT, and lamin A/C siRNA KD) cell populations to FSS. All cell types were labeled with a cell viability dye (calcein-AM), exposed to FSS, and immediately placed back into culture for ~18 h. Viability was determined via flow cytometry by number of cells expressing calcein-AM. WSS = 5,920 dyn/cm^2. Values are means ± SE of three independent measurements. *$P < 0.05$. **$P < 0.01$.

(2, 19, 52, 62); however, few studies have investigated such effects in tumor and epithelial cells. To characterize the mode of cell death induced by exposure to elevated FSS pulses, MDA-MB-231 tumor cells and MCF10A epithelial cells were placed into culture for 2 h after FSS exposure and then labeled with an annexin-V/PI viability kit to assess for cellular apoptosis and necrosis via flow cytometry. Under static conditions, MDA-MB-231 (Fig. 2*A*) and MCF10A (Fig. 2*B*) cells remained generally viable, as determined using the annexin-V/PI assay. After FSS pulse exposure, the viable population of MDA-MB-231 (Fig. 2*C*) and MCF10A (Fig. 2*D*) cells both decreased, with increased apoptotic and necrotic populations in both cell lines. On further characterization, it was found that FSS pulses significantly decreased MCF10A viability and significantly increased both cellular apoptosis and necrosis compared with MDA-MB-231 cells (Fig. 2, *E–G*). These results suggest that FSS pulses decrease tumor and epithelial cell viability via increased cellular apoptosis and necrosis, and that breast cancer cells are more resistant to FSS-induced apoptosis and necrosis than mammary epithelial cells.

Lamin A/C knockdown reduces tumor cell resistance to FSS-induced death. To assess the contribution of lamin A/C in tumor cell resistance to FSS-induced death, lamin A/C-deficient MDA-MB-231 cell lines were generated using both shRNA (Fig. 3*A*) and siRNA (Fig. 3*B*). Heterogeneous and clonal populations of stable lamin A/C knockdown MDA-MB-231 cells were generated, and lamin A/C knockdown was confirmed using Western blot analysis (Fig. 3*A*). Additionally, lamin A/C was successfully knocked down in MDA-MB-468 and MDA-MB-231 cell lines using siRNA (Fig. 3*B*). Knockdown was specific to lamin A/C in all cell types, as MDA-MB-231 and MDA-MB-468 cells retained lamin B1 but were deficient of lamin A/C, as determined by immunofluorescence (Fig. 3, *C* and *D*). Knockdown of lamin A/C using shRNA (Fig. 4*A*) and siRNA (Fig. 4*C*) had no significant effect on MDA-MB-231 and MDA-MB-468 breast cancer cell viability in the absence of FSS. However, after exposure to 10 consecutive pulses of elevated FSS, lamin A/C-depleted MDA-MB-231 cells were significantly less viable than nontargeting shRNA controls (Fig. 4*B*). This result was observed in both heterogeneous and clonal MDA-MB-231 lamin A/C knockdown populations; however, the clonal population showed lower viability (~30%) than the heterogeneous population (~50%). This is consistent with greater lamin A/C depletion in the clonal population compared with the heterogeneous population, as determined via Western blot and immunofluorescence (Fig. 3, *A* and *C*). Similar results were observed in MDA-MB-468 and MDA-MB-231 cells following siRNA-

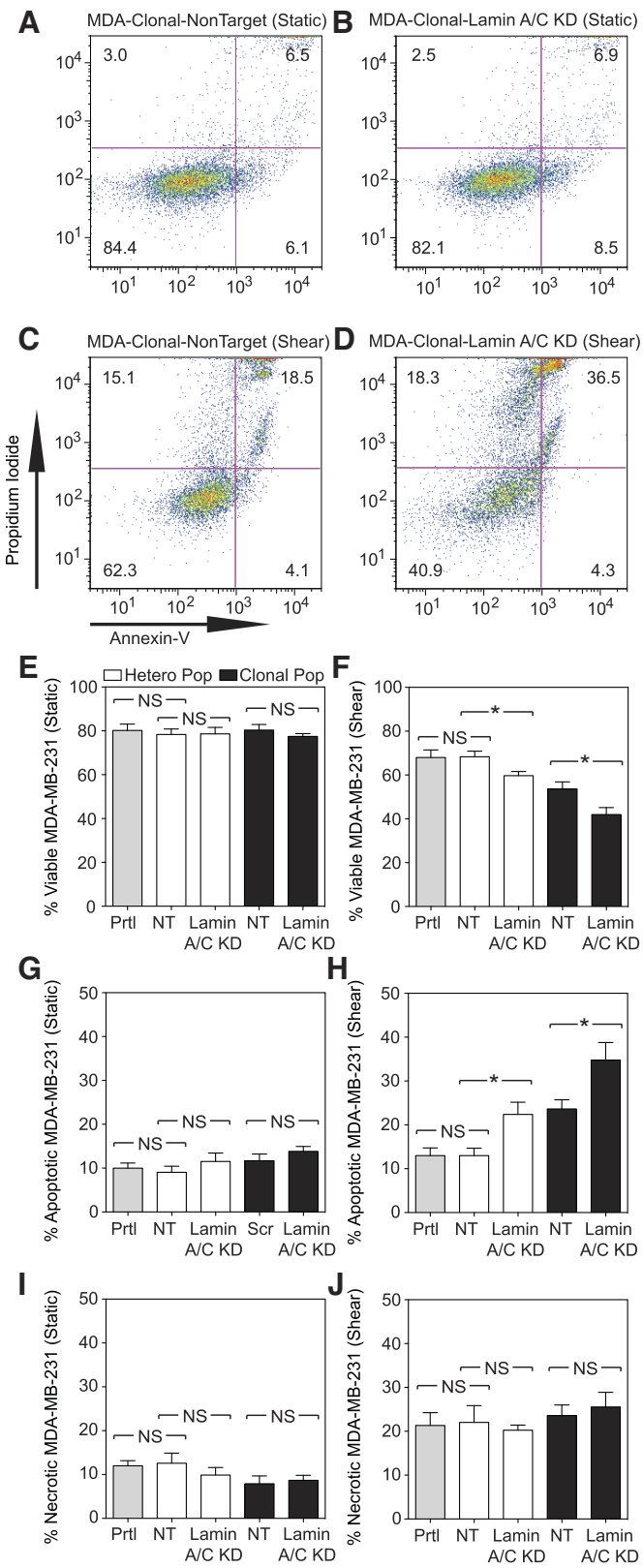

Fig. 5. Exposure to FSS induces increased apoptotic cell death in lamin A/C-deficient MDA-MB-231 tumor cells. Cells were exposed to 10 pulses of elevated FSS (WSS = 5,920 dyn/cm^2), placed back into culture for 2 h, and assessed for apoptosis and necrosis using an annexin-V/PI assay. *A–D*: annexin-V/PI flow cytometry plots of NT (*A* and *C*) and lamin A/C-deficient (*B* and *D*) MDA-MB-231 cells derived from a Clonal Pop, exposed to static conditions (*A* and *B*) and millisecond pulses of FSS (*C* and *D*). *Bottom left* quadrant (annexin-V negative, PI negative) denotes viable cells. *Top left* quadrant (annexin-V negative, PI positive) denotes necrotic cells. *Bottom right* quadrant (annexin-V positive, PI negative) denotes early-apoptotic cells. *Top right* quadrant (annexin-V positive, PI positive) denotes late-apoptotic cells. *E* and *F*: percentage of viable MDA-MB-231 cells after exposure to static conditions (*E*) or 10 pulses of elevated FSS (*F*). *G* and *H*: percentage of apoptotic MDA-MB-231 cells after exposure to static conditions (*G*) or 10 pulses of elevated FSS (*H*). *I* and *J*: percentage of necrotic MDA-MB-231 cells after exposure to static conditions (*I*) or 10 pulses of elevated FSS (*J*). Values are means ± SE of three independent measurements. *$P < 0.05$.

mediated knockdown of lamin A/C (Fig. 4, *C* and *D*). These results suggest that lamin A/C knockdown reduces MDA-MB-231 cancer cell resistance to FSS-mediated cell death.

Decreased tumor cell resistance to FSS-induced death via lamin A/C knockdown is FSS-pulse dependent. To assess how increasing the number of FSS pulses affects tumor cell death after lamin A/C knockdown, lamin A/C knockdown MDA-MB-231 and MDA-MB-468 cancer cells were exposed to a number of FSS pulses, ranging from 2–10 pulses, with 90 s in between consecutive pulses, and then assessed for viability via calcein-AM dye retention and flow cytometry quantification. No significant difference in viability in the heterogeneous population of shRNA-mediated lamin A/C knockdown cancer cells was observed after two and four consecutive pulses of FSS, compared with nontargeted heterogeneous and parental controls (Fig. 4*E*). Significant decreases in viability in the heterogeneous population of lamin A/C knockdown cells were observed after exposure to six pulses of elevated FSS or greater (Fig. 4*E*). A significant decrease in viability in the clonal population of shRNA-mediated lamin A/C knockdown cells was observed after as few as four pulses of FSS, compared with nontargeted clonal and parental controls (Fig. 4*F*). A significant decrease in the viability of siRNA-mediated lamin A/C knockdown MDA-MB-468 and MDA-MB-231 cells was observed after exposure to six pulses of FSS, compared with controls (Fig. 4, *G* and *H*).

The larger decrease in resistance in the lamin A/C knockdown clonal population after FSS exposure is likely due to the fact that minimal residual lamin A/C was detected after shRNA knockdown in the clonal population (Fig. 3, *A* and *C*). Given that a fraction of lamin A/C was still detectable after shRNA knockdown in the heterogeneous population (Fig. 3*A*), and that a subpopulation of MDA-MB-231 cells still expressed lamin A/C based on immunofluorescence analysis (Fig. 3*C*), it is likely that there is a subpopulation of cells capable of withstanding FSS pulses in the heterogeneous cell population. This would explain why the decreased resistance to FSS in the MDA-MB-231 lamin A/C heterogeneous population is less pronounced than that within the clonal counterpart (Fig. 4, *E* and *F*). These results suggest that decreased resistance to FSS-induced death of lamin A/C knockdown MDA-MB-231 cancer cells is FSS pulse dependent.

Lamin A/C knockdown increases FSS-induced tumor cell apoptosis. To characterize the mode of lamin A/C knockdown tumor cell death induced by exposure to elevated FSS pulses, both clonal and heterogeneous populations of lamin A/C knockdown MDA-MB-231 cells were placed into culture for 2 h after FSS pulse exposure and then labeled with an annexin-V/PI viability kit to assess for cellular apoptosis and necrosis via flow cytometry. Under static conditions, the viability of the nontargeted (>84%) and lamin A/C knockdown (>82%) clonal populations of MDA-MB-231 cancer cells remained generally high (Fig. 5, *A* and *B*). As anticipated, the nontargeted clonal population of MDA-MB-231 cells decreased in viability (~62%) and increased in cellular apoptosis and necrosis (Fig. 5*C*). After lamin A/C knockdown, a greater decrease MDA-MB-231 cancer viability was observed (~40%) compared with nontargeted controls. Interestingly, the decrease in viability was largely due to increased rates of apoptosis, which increased from ~22 to ~41% (Fig. 5*D*), while minimal changes were observed in cellular necrosis. Upon comparison of the parental, heterogeneous, and clonal populations, no significant differences were observed in terms of viability (Fig. 5*E*), apoptosis (Fig. 5*G*), or necrosis (Fig. 5*I*) under static conditions. Annexin-V/PI assay confirmed the calcein-AM results, showing decreased viability in lamin A/C knockdown cancer cells from both clonal and heterogeneous populations after FSS exposure, compared with nontargeted and parental controls (Fig. 5*F*). These differences in viability were due to cellular apoptosis, which was significantly increased in lamin A/C knockdown MDA-MB-231 cancer cells from both clonal and heterogeneous populations after FSS exposure, compared with nontarget and parental controls (Fig. 5*H*). However, no significant differences in cellular necrosis were observed across all populations after exposure to FSS (Fig. 5*J*). These results suggest that lamin A/C depletion reduces MDA-MB-231 tumor cell resistance to FSS-induced cell death by specifically increasing tumor cell apoptosis. It is important to note that the differences in viability found in the annexin-V/PI assay are not as pronounced as those found using calcein-AM viability staining, due to the fact that calcein-AM viability measurements were not taken until after samples were incubated overnight (~18 h), whereas annexin-V/PI measurements were conducted only 2 h after FSS exposure to ensure detection of early-apoptotic events, which typically occur within hours after tumor cells are exposed to a stimulus to trigger apoptosis (25, 35, 66).

DISCUSSION

The present study shows that lamin A/C is critical for tumor cells to withstand fluid shear forces in vitro and could play a key role in allowing CTCs to withstand FSS in the circulation. This is the first demonstration that lamin A/C promotes cell survival under FSS, expanding on previous reports that depletion of lamin A can reduce the survival of tumor cells under the

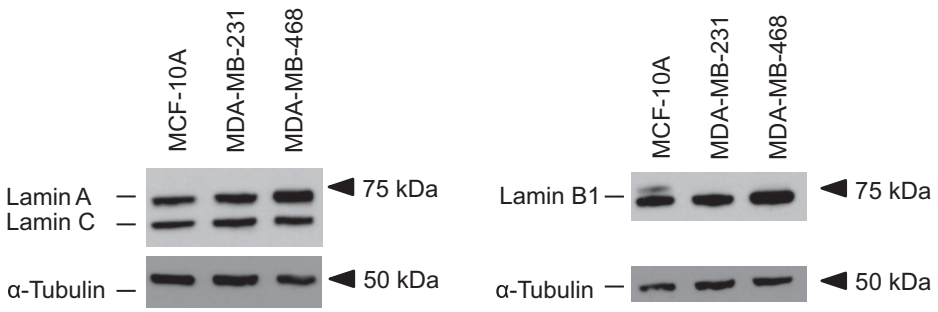

Fig. 6. Western blot of lamin A/C expression in nontreated MCF-10A, MDA-MB-231, and MDA-MB-468 cells.

stress of three-dimensional migration (24), and that lamin A/C-deficient cells undergo significantly increased apoptosis under mechanical strain, compared with wild-type fibroblasts (33). While our results suggest that tumor cells with reduced levels of lamin A/C have lower rates of survival in the circulation, it is important to note that the overall role of lamin A/C in tumor progression is likely more complex, as transport in the bloodstream is just one of many steps in the metastatic cascade. For example, low levels of lamin A/C could enhance tumor cell invasion through tight interstitial spaces and ECMs during the initial stages of metastasis, as lamin A/C-deficient cells have more deformable nuclei and can move significantly faster through narrow constrictions than cells with normal lamin A/C expression (16), resulting in increased three-dimensional migration of tumor cells (24). Finally, lamins may promote metastasis through their role in transcriptional regulation (63), including their requirement for mechanically activated gene transcription (26, 33), and lamin A/C is also known to play a role in DNA repair and cell viability (20).

Future studies should explore whether the observed protective effect of lamin A/C to FSS is specific to tumor cells or generalizable to all cell types in circulation. As discussed above, functional loss of lamin A/C results in increased susceptibility to mechanical stress in a variety of cells, including lamin A/C-deficient mouse embryo fibroblast and primary human skin fibroblasts carrying dominant-negative lamin A/C mutations (33, 67). On the other hand, neutrophils, which predominantly reside in the circulation, express minimal levels of lamins (54). Therefore, the effects of lamin A/C are expected to be context dependent at the molecular level and dependent on the cell type. One reason may be that lamins bind to a large number of interaction partners within cells (27), and that the expression of these binding partners can vary between cell types. Thus it is likely that different cell types will exhibit different responses to lamin A/C depletion. In addition, perturbed signaling networks in tumor cells compared with normal cells, such as p53 mutations (5), may contribute to further differences in the effects of lamin A/C depletion.

Although it is likely that other structural components additionally contribute to increased tumor cell viability upon exposure to FSS, the pronounced differences in viability between lamin A/C knockdown and nontargeted MDA-MB-231 controls after FSS demonstrate that lamin A/C play a crucial role in providing mechanical support against such forces. While no differences in lamin A/C expression were observed between MCF10A and the two metastatic breast cancer cell lines (Fig. 6), and thus differences in sensitivity to FSS cannot be attributed to differential lamin A/C expression between tumor and noncancerous cells, our finding that decreased levels of lamin A/C result in increased sensitivity to FSS in metastatic breast cancer cells is highly relevant in the clinical setting when comparing different tumor cells. Recent work has shown that breast cancer is often associated with decreased levels of lamin A/C, and loss of lamin A/C negatively correlates with disease survival (8, 61). However, our current work shows that lamin A/C deficiency reduced tumor cell viability under shear stress conditions of the bloodstream. Taken together, these studies demonstrate that the role of lamin A/C in cancer metastasis is highly complex, with multiple, context-specific, and at times opposing functions, for example, during tissue invasion and in circulation, warranting further studies.

Conclusions. The results from this study suggest that tumor cells are resistant to elevated FSS, compared with epithelial cells, in a FSS-pulse-dependent manner. MDA-MB-231 and MDA-MB-468 breast cancer cells were found to be more resistant to both FSS-induced cellular apoptosis and necrosis, compared with MCF10A breast epithelial cells. Upon knockdown of lamin A/C, MDA-MB-231 and MDA-MB-468 cells became significantly less resistant to FSS, as evidenced by decreased viability and significantly increased apoptosis. Recent findings have reported that loss of lamins A/C can result in increased cell death as cancer cells migrate through narrow pores (24). Our results suggest that lamin A/C is also an important structural component in CTCs for withstanding hemodynamic shear forces and promoting subsequent metastasis formation. Lamin A/C may thus serve as an important biomarker for CTCs and metastatic tumors. Clinically, lamin A/C may also serve as a target for gene therapies, including siRNA delivery, to promote CTC apoptosis within the bloodstream.

GRANTS

The work described was supported by the Cornell Center on the Microenvironment and Metastasis through Award no. U54CA143876 from the National Cancer Institute (NCI). This work was supported by National Institutes of Health awards (R01 NS-059348 and R01 HL-082792); the Department of Defense Breast Cancer Idea Award (BC102152); a National Science Foundation CAREER award to J. Lammerding (CBET-1254846); and a Pilot Project Award by the Cornell Center on the Microenvironment & Metastasis through Award no. U54CA143876 from the NCI.

DISCLAIMER

The content is solely the responsibility of the authors and does not necessarily represent the official views of the National Cancer Institute or the National Institutes of Health.

DISCLOSURES

No conflicts of interest, financial or otherwise, are declared by the author(s).

AUTHOR CONTRIBUTIONS

Author contributions: M.M., J.L., and M.K. conception and design of research; M.M., C.D., M.C., and Z.W. performed experiments; M.M., C.D., M.C., and Z.W. analyzed data; M.M., C.D., J.L., and M.K. interpreted results of experiments; M.M. and C.D. prepared figures; M.M. and C.D. drafted manuscript; M.M., C.D., M.C., J.L., and M.K. edited and revised manuscript; M.M., C.D., M.C., Z.W., J.L., and M.K. approved final version of manuscript.

REFERENCES

1. **Alemu Y, Bluestein D.** Flow-induced platelet activation and damage accumulation in a mechanical heart valve: numerical studies. *Artif Organs* 31: 677–688, 2007.
2. **Bakker A, Klein-Nulend J, Burger E.** Shear stress inhibits while disuse promotes osteocyte apoptosis. *Biochem Biophys Res Commun* 320: 1163–1168, 2004.
3. **Barnes JM, Nauseef JT, Henry MD.** Resistance to fluid shear stress is a conserved biophysical property of malignant cells. *PLos One* 7: e50973, 2012.
4. **Bluestein D, Niu L, Schoephoerster RT, Dewanjee MK.** Fluid mechanics of arterial stenosis: Relationship to the development of mural thrombus. *Ann Biomed Eng* 25: 344–356, 1997.
5. **Bond GL, Hu W, Bond E, Robins H, Lutzker SG, Arva NC, Bargonetti J, Bartel F, Taubert H, Wuerl P, Onel K, Yip L, Hwang SJ, Strong LC, Lozano G, Levine AJ.** A single nucleotide polymorphism in the MDM2 promoter attenuates the p53 tumor suppressor pathway and accelerates tumor formation in humans. *Cell* 119: 591–602, 2004.
6. **Brooks DE.** The biorheology of tumor cells. *Biorheology* 21: 85–91, 1984.

7. **Cao TM, Mitchell MJ, Liesveld J, King MR.** Stem cell enrichment with selectin receptors: mimicking the pH environment of trauma. *Sensors (Basel)* 13: 12516–12526, 2013.
8. **Capo-chichi CD, Cai KQ, Smedberg J, Ganjei-Azar P, Godwin AK, Xu XX.** Loss of A-type lamin expression compromises nuclear envelope integrity in breast cancer. *Chin J Cancer* 30: 415–425, 2011.
9. **Chaffer CL, Weinberg RA.** A perspective on cancer cell metastasis. *Science* 331: 1559–1564, 2011.
10. **Chambers A, Naumov G, Vantyghem S, Tuck AB.** Molecular biology of breast metastasis: clinical implications of experimental studies on metastatic inefficiency. *Breast Cancer Res* 2: 400–407, 2000.
11. **Chambers AF, MacDonald IC, Schmidt EE, Koop S, Morris VL, Khokha R, Groom AC.** Steps in tumor metastasis: new concepts from intravital microscopy. *Cancer Metastasis Rev* 14: 279–301, 1995.
12. **Cheon GJ, Chandran KB.** Dynamic behavior analysis of mechanical monoleaflet heart valve prostheses in the opening phase. *J Biomech Eng* 115: 389–395, 1993.
13. **Clarke MS, McNeil PL.** Syringe loading introduces macromolecules into living mammalian cell cytosol. *J Cell Sci* 102: 533–541, 1992.
14. **Colantuoni G, Hellums JD, Moake JL, Alfrey CP.** The response of human platelets to shear stress at short exposure times. *Trans Am Soc Artif Intern Organs* 23: 626–631, 1977.
15. **Coussens LM, Werb Z.** Inflammation and cancer. *Nature* 420: 860–867, 2002.
16. **Davidson P, Denais C, Bakshi MC, Lammerding J.** Nuclear deformability constitutes a rate-limiting step during cell migration in 3-D environments. *Cell Mol Bioeng* 7: 293–306, 2014.
17. **Davidson PM, Lammerding J.** Broken nuclei–lamins, nuclear mechanics, disease. *Trends Cell Biol* 24: 247–256, 2014.
18. **Denais C, Lammerding J.** Nuclear mechanics in cancer. *Adv Exp Med Biol* 773: 435–470, 2014.
19. **Dimmeler S, Assmus B, Hermann C, Haendeler J, Zeiher AM.** Fluid shear stress stimulates phosphorylation of Akt in human endothelial cells: involvement in suppression of apoptosis. *Circ Res* 83: 334–341, 1998.
20. **Dittmer TA, Misteli T.** The lamin protein family. *Genome Biol* 12: 222, 2011.
21. **Fidler IJ.** Metastasis: quantitative analysis of distribution and fate of tumor emboli labeled with ^{125}I-5-Iodo-2′-deoxyuridine. *J Natl Cancer Inst* 45: 773–782, 1970.
22. **Folker ES, Ostlund C, Luxton GWG, Worman HJ, Gundersen GG.** Lamin A variants that cause striated muscle disease are defective in anchoring transmembrane actin-associated nuclear lines for nuclear movement. *Proc Natl Acad Sci U S A* 108: 131–136, 2011.
23. **Foster CR, Przyborski S, Wilson R.** Lamins as cancer biomarkers. *Biochem Soc Trans* 38: 297–300, 2010.
24. **Harada T, Swift J, Irianto J, Shin JW, Spinler KR, Athirasala A, Diegmiller R, Dingal PCDP, Ivanovska IL, Discher DE.** Nuclear lamin stiffness is a barrier to 3D migration, but softness can limit survival. *J Cell Biol* 204: 669–682, 2014.
25. **Hirsch T, Marchetti P, Susin SA, Dallaporta B, Zamzami N, Marzo I, Geuskens M, Kroemer G.** The apoptosis-necrosis paradox. Apoptogenic proteases activated after mitochondrial permeability transition determine the mode of cell death. *Oncogene* 15: 1573–1581, 1997.
26. **Ho CY, Jaalouk DE, Vartiainen MK, Lammerding J.** Lamin A/C and emerin regulate MKL1-SRF activity by modulating actin dynamics. *Nature* 497: 507–511, 2013.
27. **Ho CY, Lammerding J.** Lamins at a glance. *J Cell Sci* 125: 2087–2093, 2012.
28. **Hughes AD, King MR.** Nanobiotechnology for the capture and manipulation of circulating tumor cells. *Wiley Interdiscip Rev Nanomed Nanobiotechnol* 4: 291–309, 2011.
29. **Hughes AD, Marshall JR, Keller E, Powderly JD, Greene BT, King MR.** Differential drug responses of circulating tumor cells within patient blood. *Cancer Lett* 352: 28–35, 2014.
30. **Isermann P, Lammerding J.** Nuclear mechanics and mechanotransduction in health and disease. *Curr Biol* 23: R1113–R1121, 2013.
31. **Kandlikar S, Garimella S, Li D, Colin S, King MR.** *Heat Transfer and Fluid Flow in Minichannels and Microchannels*. Atlanta, GA: Elsevier, 2005.
32. **Lammerding J, Fong LG, Ji JY, Reue K, Stewart CL, Young SG, Lee RT.** Lamins A and C but not lamin B1 regulate nuclear mechanics. *J Biol Chem* 281: 25768–25780, 2006.
33. **Lammerding J, Schulze PC, Takahashi T, Kozlov S, Sullivan T, Kamm RD, Stewart CL, Lee RT.** Lamin A/C deficiency causes defective nuclear mechanics and mechanotransduction. *J Clin Invest* 113: 370–378, 2004.
34. **Las Heras de JI, Batrakou DG, Schirmer EC.** Cancer biology and the nuclear envelope: a convoluted relationship. *Semin Cancer Biol* 23: 125–137, 2013.
35. **Logue SE, Elgendy M, Martin SJ.** Expression, purification and use of recombinant annexin V for the detection of apoptotic cells. *Nat Protoc* 4: 1383–1395, 2009.
36. **Luxton GWG, Gomes ER, Folker ES, Worman HJ, Gundersen GG.** TAN lines: a novel nuclear envelope structure involved in nuclear positioning. *Nucleus* 2: 173–181, 2011.
37. **MacDonald IC, Groom AC, Chambers AF.** Cancer spread and micrometastasis development: Quantitative approaches for in vivo models. *Bioessays* 24: 885–893, 2002.
38. **Malek AM, Alper SL, Izumo S.** Hemodynamic shear stress and its role in atherosclerosis. *JAMA* 282: 2035–2042, 1999.
39. **Mehlen P, Puisieux A.** Metastasis: a question of life or death. *Nat Rev Cancer* 6: 449–458, 2006.
40. **Michor F, Liphardt J, Ferrari M, Widom J.** What does physics have to do with cancer? *Nat Rev Cancer* 11: 657–670, 2011.
41. **Mitchell MJ, Castellanos CA, King MR.** Nanostructured surfaces to target and kill circulating tumor cells while repelling leukocytes. *J Nanomater* 2012: 1–10, 2012.
42. **Mitchell MJ, Castellanos CA, King MR.** Immobilized surfactant-nanotube complexes support selectin-mediated capture of viable circulating tumor cells in the absence of capture antibodies. *J Biomed Mater Res A* 103A: 3407–3418, 2015.
43. **Mitchell MJ, Castellanos CA, King MR.** Surfactant functionalization induces robust, differential adhesion of tumor cells and blood cells to charged nanotube-coated biomaterials under flow. *Biomaterials* 56: 179–186, 2015.
44. **Mitchell MJ, Chen CS, Ponmudi V, Hughes AD, King MR.** E-selectin liposomal and nanotube-targeted delivery of doxorubicin to circulating tumor cells. *J Control Release* 160: 609–617, 2012.
45. **Mitchell MJ, King MR.** Shear-induced resistance to neutrophil activation via the formyl peptide receptor. *Biophys J* 102: 1804–1814, 2012.
46. **Mitchell MJ, King MR.** Fluid shear stress sensitizes cancer cells to receptor-mediated apoptosis via trimeric death receptors. *New J Phys* 15: 015008, 2013.
47. **Mitchell MJ, King MR.** Computational and experimental models of cancer cell response to fluid shear stress. *Front Oncol* 3: 1–11, 2013.
48. **Mitchell MJ, King MR.** Physical biology in cancer. 3. The role of cell glycocalyx in vascular transport of circulating tumor cells. *Am J Physiol Cell Physiol* 306: C89–C97, 2014.
49. **Mitchell MJ, Lin KS, King MR.** Fluid shear stress increases neutrophil activation via platelet-activating factor. *Biophys J* 106: 2243–2253, 2014.
50. **Mitchell MJ, Wayne E, Rana K, Schaffer CB, King MR.** TRAIL-coated leukocytes that kill cancer cells in the circulation. *Proc Natl Acad Sci U S A* 111: 930–935, 2014.
51. **Ostlund C, Folker ES, Choi JC, Gomes ER, Gundersen GG, Worman HJ.** Dynamics and molecular interactions of linker of nucleoskeleton and cytoskeleton (LINC) complex proteins. *J Cell Sci* 122: 4099–4108, 2009.
52. **Pavalko FM, Gerard RL, Ponik SM, Gallagher PJ, Jin Y, Norvell SM.** Fluid shear stress inhibits TNF-alpha-induced apoptosis in osteoblasts: a role for fluid shear stress-induced activation of PI3-kinase and inhibition of caspase-3. *J Cell Physiol* 194: 194–205, 2003.
53. **Pedersen JA, Boschetti F, Swartz MA.** Effects of extracellular fiber architecture on cell membrane shear stress in a 3D fibrous matrix. *J Biomech* 40: 1484–1492, 2007.
54. **Rowat AC, Jaalouk DE, Zwerger M, Ung WL, Eydelnant IA, Olins DE, Olins AL, Herrmann H, Weitz DA, Lammerding J.** Nuclear envelope composition determines the ability of neutrophil-type cells to passage through micron-scale constrictions. *J Biol Chem* 288: 8610–8618, 2013.
55. **Strony J, Beaudoin A, Brands D, Adelman B.** Analysis of shear stress and hemodynamic factors in a model of coronary artery stenosis and thrombosis. *Am J Physiol Heart Circ Physiol* 265: H1787–H1796, 1993.
56. **Swartz MA, Fleury ME.** Interstitial flow and its effects in soft tissues. *Annu Rev Biomed Eng* 9: 229–256, 2007.
57. **Swartz MA, Lund AW.** Lymphatic and interstitial flow in the tumour microenvironment: linking mechanobiology with immunity. *Nat Rev Cancer* 12: 210–219, 2012.

58. **Tarbell JM, Weinbaum S, Kamm RD.** Cellular fluid mechanics and mechanotransduction. *Ann Biomed Eng* 33: 1719–1723, 2005.
59. **Terasaki M, Miyake K, McNeil PL.** Large plasma membrane disruptions are rapidly resealed by Ca2+-dependent vesicle-vesicle fusion events. *J Cell Biol* 139: 63–74, 1997.
60. **Turitto VT.** Blood viscosity, mass transport, thrombogenesis. *Prog Hemost Thromb* 6: 139–177, 1982.
61. **Wazir U, Ahmed MH, Bridger JM, Harvey A, Jiang WG, Sharma AK, Mokbel K.** The clinicopathological significance of lamin A/C, lamin B1 and lamin B receptor mRNA expression in human breast cancer. *Cell Mol Biol Lett* 18: 595–611, 2013.
62. **Weber M, Baker MB, Moore JP, Searles CD.** MiR-21 is induced in endothelial cells by shear stress and modulates apoptosis and eNOS activity. *Biochem Biophys Res Commun* 393: 643–648, 2010.
63. **Willis ND, Cox TR, Rahman-Casans SF, Smits K, Pryzborski SA, van den Brandt P, van Engeland M, Weijenberg M, Wilson RG, de Bruine A, Hutchison CJ.** Lamin A/C is a risk biomarker in colorectal cancer. *PLos One* 3: e2988, 2008.
64. **Wirtz D, Konstantopoulos K, Searson PC.** The physics of cancer: the role of physical interactions and mechanical forces in metastasis. *Nat Rev Cancer* 11: 512–522, 2011.
65. **Zeidman I, McCutcheon M, Coman DR.** Factors affecting the number of tumor metastases; experiments with a transplantable mouse tumor. *Cancer Res* 10: 357–359, 1950.
66. **Zhao W, Mackenzie GG, Murray OT, Zhang Z, Rigas B.** Phosphoaspirin (MDC-43), a novel benzyl ester of aspirin, inhibits the growth of human cancer cell lines more potently than aspirin: a redox-dependent effect. *Carcinogenesis* 30: 512–519, 2009.
67. **Zwerger M, Jaalouk DE, Lombardi ML, Isermann P, Mauermann M, Dialynas G, Herrmann H, Wallrath LL, Lammerding J.** Myopathic lamin mutations impair nuclear stability in cells and tissue and disrupt nucleo-cytoskeletal coupling. *Hum Mol Genet* 22: 2335–2349, 2013.